Expression of flagella is coincident with uropathogenic *Escherichia coli* ascension to the upper urinary tract

M. Chelsea Lane, Christopher J. Alteri, Sara N. Smith, and Harry L. T. Mobley*

Department of Microbiology and Immunology, University of Michigan Medical School, Ann Arbor, MI 48109-0620

Uropathogenic *Escherichia coli* (UPEC) cause most uncomplicated urinary tract infections (UTIs) in humans. Because UTIs are considered to occur in an ascending manner, flagellum-mediated motility has been suggested to contribute to virulence by enabling UPEC to disseminate to the upper urinary tract. Previous studies from our laboratory and others have demonstrated a modest yet important role for flagella during ascending UTI. To better understand the role of flagella *in vivo*, we used biophotonic imaging to monitor UPEC infection and temporospatial flagellin gene expression during ascending UTI. Using *em7-lux* (constitutive) and *fliC-lux* transcriptional fusions, we show that flagellin expression by UPEC coincides with ascension of the ureters and colonization of the kidney. The patterns of *fliC* luminescence observed *in vitro* and *in vivo* were also validated by comparative quantitative PCR. Because *fliC* expression appeared coincident during ascension, we reassessed the contribution of *fliC* to ascending UTI using a low-dose intraurethral model of ascending UTI. Although wild-type UPEC were able to establish infection in the bladder and kidneys by 6 hours postinoculation, *fliC* mutant bacteria were able to colonize the bladder but were significantly attenuated in the kidneys at this early time point. By 48 hours postinoculation, the *fliC* mutant bacteria were attenuated in the bladder and kidneys and were not detectable in the spleen. These data provide compelling evidence that wild-type UPEC express flagellin and presumably utilize flagellum-mediated motility during UTI to ascend to the upper urinary tract and disseminate within the host.

biophotonic imaging | urinary tract infection | pyelonephritis | motility | fliC

It has been hypothesized that flagella, organelles required for motility, facilitate the establishment and spread of infection by microbial pathogens within the host (1, 2). Studies suggest that up to 95% of urinary tract infections (UTIs) develop in an ascending manner (3) beginning with periurethral colonization by bacteria such as uropathogenic *Escherichia coli* (UPEC), followed by migration to the bladder to establish infection, and if left untreated, ascension to the upper urinary tract or ureters and kidneys (4). Once in the kidneys, UPEC can gain access to the bloodstream, causing bacteremia and sometimes death (5). Because UTIs caused by UPEC are ascending infections involving multiple organs, we reasoned that monitoring flagella expression during UTI in real time would be useful as a model system to examine the connection between motility and the establishment and spread of bacterial infection.

The bacterial flagellum is a long helical surface appendage composed of polymerized subunits of flagellin encoded by *fliC*. Mutation of *fliC* in UPEC leads to loss of flagellation and motility. Recently, our laboratory and others showed that *fliC* mutants were out-competed by motile wild-type strains during experimental cochallenge of mice, demonstrating that flagella contribute to the efficient colonization of the urinary tract (6, 7). The limitation of these challenge experiments was the inability to define the precise location and time flagella are expressed *in vivo* to provide the wild-type strain with the fitness advantage. Using a DNA microarray for UPEC strain CFT073, our laboratory previously determined the transcriptional profile of CFT073 during ascending UTI in CBA/J mice (8). We demonstrated that, overall, genes involved in flagellum-mediated motility and chemotaxis were down-regulated *in vivo* when compared with *in vitro* growth conditions (8). Although this study provided important insight into the *in vivo* transcriptome of UPEC during ascending UTI, data represented averages of expression over a 10-day period. Thus, using transcriptional profiling, it is possible neither to assess the level of transient expression for flagellin or any given gene nor to determine the specific tissue in which this expression occurred.

For some bacterial pathogens such as pandemic *Vibrio cholerae* strains, motility mutants are highly attenuated *in vivo* (9). In others, such as *Salmonella enterica* serovar Typhimurium, *fliC* is expressed during invasion through Peyer's Patches but not in the mesenteric lymph nodes or spleen to promote escape from immune responses and to spread to systemic sites of replication (10). Because much attention has been focused on immune recognition of bacterial flagellin via Toll-like receptor 5 (11–13), and it is unknown how flagella contribute to ascending infections, it would be advantageous to assess the spatial and temporal expression of UPEC flagellin in real time during UTI. Noninvasive biophotonic imaging has been used for real-time monitoring of organism density and spread in various animal models of infection, including UTI caused by *Pseudomonas aeruginosa* and *Proteus mirabilis* (14–16). This technology has also been used to measure gene-specific real-time expression of a global virulence regulator, *agr*, during *Staphylococcus aureus* s.c. abscess formation (17).

Here we used noninvasive biophotonic imaging to assess the level and site of flagellar gene expression during ascending infection and to resolve the fitness advantage flagella provide UPEC *in vivo*. A luminescent *fliC* reporter plasmid was constructed that was stably maintained *in vivo* and demonstrated flagellin-specific patterns of luminescence during swimming and swarming *in vitro*. Using this construct, we found that *fliC* expression coincided with bacterial ascension to the upper urinary tract, showing that motility is involved in the migration of the infection from the bladder to the kidneys. The *in vivo* expression of *fliC* was verified by quantitative PCR (qPCR), and the contribution of *fliC* to ascending infection was reassessed by using a low-dose intraurethral inoculation model

MICROBIOLOGY

(18). Although wild-type UPEC were able to ascend the urethra to the bladder and migrate to the kidneys, *fliC* mutant bacteria were significantly less able to reach the upper urinary tract.

Results

Construction of a Bioluminescent *fliC* Reporter and Correlation of Expression with Motility. All bioluminescence reporters were expressed in UPEC strain CFT073 (O6:K2:H1), which was isolated from the blood of a hospitalized patient with acute pyelonephritis (19). The *luxCDABE* gene cluster encoding bacterial luciferase [isolated from pUT-Tn5-EM7-*lux*-Km1 (20), a generous gift from C. Contag, Stanford University, Palo Alto, CA] was cloned into the low-copy plasmid pGEN222 [ref. 21; a gift from J. Galen (University of Maryland, Baltimore] [supporting information (SI) Fig. 4 and SI Table 1]. The resulting plasmid, pGEN-*luxCDABE*, carries the synthetic *em7* promoter that drives constitutive expression of the *luxCDABE* operon and is referred to as P$_{em7}$-*lux*. P$_{em7}$-*lux* retains the novel plasmid maintenance system from pGEN222, with the *hok sok* postsegregation killing system and two *par* (partitioning) loci to enhance plasmid stability over multiple bacterial generations (ref. 21; SI Fig. 4 and SI Table 1). The maintenance of P$_{em7}$-*lux* was assessed *in vitro* in the absence of antibiotic pressure by examining the loss of antibiotic resistance of CFT073 cultured statically at 37°C and subcultured every 24 h for 3 days. After 1 and 3 days of passaging, the plasmid appeared relatively stable in the absence of antibiotics in that 97.8% and 86.6% of the CFT073 population, respectively, retained P$_{em7}$-*lux* (SI Fig. 5).

To create the bioluminescent *fliC* reporter, the *em7* promoter of P$_{em7}$-*lux* was replaced with a 244-bp fragment that includes the *fliC* promoter of CFT073 (SI Fig. 4) (7, 22). The resulting construct, P$_{fliC}$-*lux*, was transformed into CFT073. Unlike the P$_{em7}$-*lux* transformants, CFT073 transformants containing the P$_{fliC}$-*lux* reporter expressed *lux* as a halo concentrated at the periphery of colonies on LB agar (Fig. 1A). *In vitro* growth rates of CFT073 containing the P$_{em7}$-*lux* or P$_{fliC}$-*lux* reporters were comparable and *lux* expression from the P$_{em7}$-*lux* reporter was constitutive (Fig. 1B). Levels of *lux* expression from the P$_{fliC}$-*lux* reporter, however, corresponded to changing levels of motility observed by phase-contrast microscopy (Fig. 1B). As predicted, peak P$_{fliC}$-*lux* activity preceded the maximal motility of the culture at early exponential phase (OD$_{600}$ = 0.3) (Fig. 1B, arrow), presumably because of the length of time required to assemble the complex flagellar apparatus after transcription of the class III genes.

To further correlate motility and expression of the P$_{fliC}$-*lux* reporter, we examined the pattern of luminescence displayed by the *fliC* and *em7* reporters while swimming in 0.25% agar or swarming atop 0.45% agar (Fig. 1C). To demonstrate the level of background luminescence *in vitro*, we also measured the luminescence of CFT073 containing P$_{neg}$-*lux*, a promoterless control reporter, during motility in 0.25% agar. Overnight cultures of the P$_{fliC}$-*lux*, P$_{em7}$-*lux* and P$_{neg}$-*lux* reporters were recultured in fresh LB, standardized to an OD$_{600}$ = 1.0, and then either stabbed into 0.25% tryptone agar or spotted (5 μl) onto 0.45% Eiken agar. The swimming and swarming plates were incubated for 16 h at 30°C and 37°C, respectively. Although all three reporters formed similar motility patterns, the patterns of luminescence displayed were distinct (as demonstrated by the density plots to the right of the luminescence images in Fig. 1C). As expected, the level of *in vitro lux* expression by P$_{neg}$-*lux* was not detectable by the ChemiDoc XRS system (Bio-Rad, Hercules, CA) (Fig. 1C). The pattern of luminescence exhibited by the P$_{em7}$-*lux* reporter correlated with the concentration of the bacterial population; the more bacteria present, the brighter the luminescence (which was expected with the constitutive *lux* reporter) (Fig. 1C). In contrast, the pattern of P$_{fliC}$-*lux* luminescence was brightest at the outer ring of motility in 0.25% agar and along the outer edge of the swarm atop 0.45% agar (Fig. 1C). This phenomenon is consistent with previous observations that FliC expression, and overall flagella production are
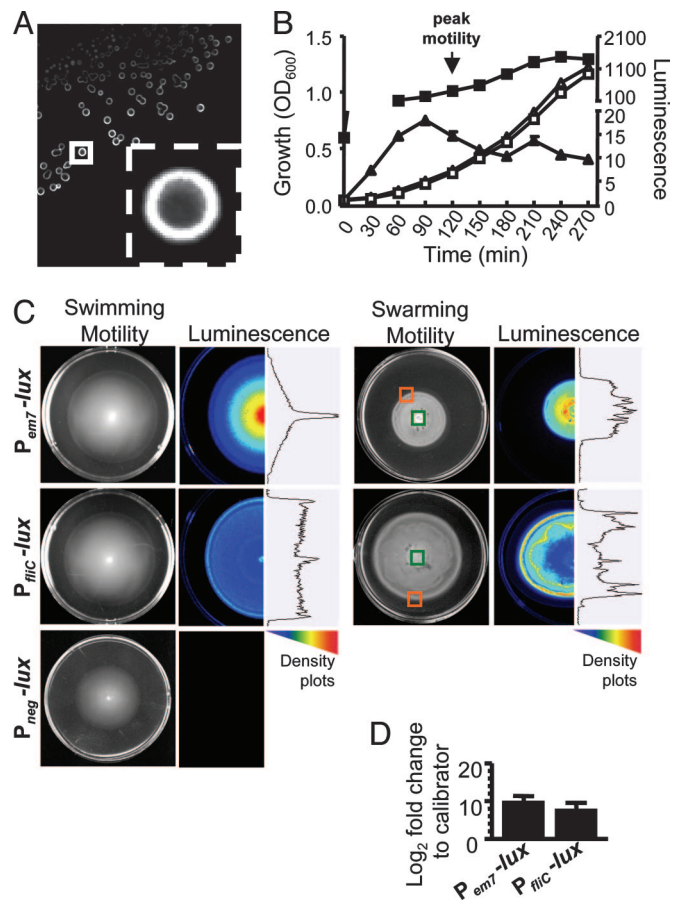

Fig. 1. *In vitro* characterization of wild-type CFT073 P$_{fliC}$-*lux* and P$_{em7}$-*lux* reporters. (*A*) Luminescence of wild-type CFT073 transformants containing the P$_{fliC-[infi]lux}$ reporter. (*Inset*) Enlargement of boxed colony. (*B*) Growth and luminescence expression of P$_{fliC}$-*lux* (△ and ▲, respectively) and P$_{em7}$-*lux* (□ and ■, respectively). Average (*n* = 3) optical densities and luminescence were plotted. Arrow indicates the highest level of motility as observed by phase-contrast microscopy. (*C*) Motility and luminescence images of P$_{fliC}$-*lux*, P$_{em7}$-*lux*, and P$_{neg}$-*lux* reporters swimming within 0.25% tryptone agar (*Left*) or swarming atop 0.45% Eiken agar (*Right*). Cultures of each reporter were stabbed into soft agar plates or spotted atop swarm plates and incubated for 16 h at 30°C or 37°C, respectively. (*D*) qPCR analysis of *fliC* transcription within the inside and outer edge of swarms formed by the P$_{fliC}$-*lux* and P$_{em7}$-*lux* reporters. Black bars represent the average changes (log$_2$-fold; *n* = 3) in expression of *fliC* between the inside (green boxes in *C*) and outer edge (orange boxes in *C*) of the swarms. Error bars represent the standard error of the mean.

maximal along the edge of *E. coli* swarm fronts (23). Here, we also demonstrated by comparative qPCR that the amount of *fliC* transcription along the outer edge of the swarms produced by P$_{fliC}$-*lux* and P$_{em7}$-*lux* were approximately log$_2$ 8.0-fold (256-fold) and log$_2$ 10.1-fold (1,098-fold) greater, respectively, than the bacteria residing in the center of the swarms (Fig. 1D). It is important to note, however, that only the luminescence profile of the P$_{fliC}$-*lux* reporter correlates with the pattern of *fliC* transcription observed in the swarm assays (Fig. 1 *C* and *D*).

Temporal and Spatial Expression of *fliC* in Vivo. Before examining the temporospatial expression of *fliC*, the progression of UPEC infection was monitored by imaging mice infected with the constitutive CFT073 P$_{em7}$-*lux* reporter using the *in vivo* imaging system, IVIS 200 (Xenogen, Hopkinton, MA). Preliminary studies conducted in our laboratory demonstrated that, on average, 99.3% of the CFT073 population retained the P$_{em7}$-*lux* reporter plasmid after 48 h *in vivo* (from both the bladder and kidneys; data not shown).

Once the *in vivo* stability of the P_{em7}-*lux* reporter was confirmed, we monitored the progression of ascending UTI by biophotonic imaging and demonstrated that the luminescence observed is indicative of bacterial infection within the lower (bladder) and/or upper (kidneys) urinary tract. Indeed, the luminescence emitted from regions of interest (ROIs) positively correlated ($P < 0.0001$) with the number of viable bacteria harvested from the kidneys at 48 hpi for the constitutive *em7* reporter (data not shown). Additionally, as we monitored the progression of infection, we were able to demonstrate that the bladders and kidneys, which appeared to be bioluminescent *in vivo*, were also bioluminescent *ex vivo* (SI Fig. 6). The enzymatic activity of bacterial luciferase required oxygen, as demonstrated by the disappearance of the luminescent signals emitted from the ROIs within 5 min after death [most likely due to the loss of circulating oxygenated blood to the tissues as described by Wiles *et al.* (24) (data not shown)]. Furthermore, we observed luminescence from the kidney *ex vivo* only when it was minced into small pieces allowing oxygenation (SI Fig. 6). It is not surprising that the bladder is extremely luminescent *ex vivo*, because after harvesting the organ, it acquired a large opening that exposed the lumen of the bladder to air (SI Fig. 6).

To more closely monitor the progression of CFT073 infection during the earliest time points of UTI ascension, 10^9 cfu of CFT073 containing P_{em7}-*lux* were inoculated into the bladders of 20 CBA/J mice, respectively. To demonstrate that *em7* reporter luminescence was significantly higher than background, an additional 14 CBA/J mice were monitored that were infected with CFT073 containing P_{neg}-*lux*. From 2 to 9 h postinoculation (hpi), mice were imaged hourly by using the IVIS 200, and luminescence was acquired and quantified in the bladder and kidneys using the Living Image software (Xenogen). Images of a representative mouse infected over time with CFT073 containing the constitutive P_{em7}-*lux* reporter are presented in Fig. 2*A*. In Fig. 2*A*, the scale is demonstrating luminescence emission per individual pixel and not total luminescence of a region of interest as indicated by the scatter plots in Fig. 2 *C* and *D*. The amount of luminescence emitted from the bladder from 2 to 9 hpi by CFT073 containing the constitutive *em7* reporter remained for the most part unchanged and significant over background (Fig. 2 *A* Ventral and *D*), suggesting that the colonization of bladder by UPEC remains at a steady state during early time points of infection. In contrast, the amount of luminescence emitted from the kidneys steadily increased from 2 to 9 hpi (it was, however, significant over background at all early time points with the exception of the 2-h time point in the right kidney) (Fig. 2 *A* Dorsal and *C*). Moreover, during some of the early time points on the ventral side of the mice, it is possible to observe a trail of luminescent signal with the constitutive reporter leading from the bladder to the right kidney on the ventral side of the mice (Fig. 2*A* Ventral). Altogether, these data illustrate that, although the bladder retains a steady state of UPEC colonization, there is a gradual ascension of UPEC from the bladder to the kidneys, which causes an increase in luminescence signal as UPEC colonizes the kidneys. Because we have been able to culture UPEC from the ureters during ascending murine infection (data not shown), it is likely that the route of ascension from the bladder to the kidneys is through the ureters.

To determine the temporospatial expression of *fliC* during early bladder colonization and ascension to the upper urinary tract, 19 additional CBA/J mice were transurethrally inoculated with 10^9 cfu of CFT073 containing P_{fliC}-*lux* and imaged every hour from 2 to 9 hpi. It is important to note that wild-type CFT073 containing each of the P_{em7}-*lux*, P_{neg}-*lux*, and P_{fliC}-*lux* equally colonized the urinary tract at 9 hpi, because the cfus per gram of bladder or kidney tissue did not significantly differ (data not shown). Images of a representative mouse infected over time with CFT073 containing the constitutive P_{fliC}-*lux* reporter are presented in Fig. 2*A*. In contrast to the constitutive luminescence observed over time in the bladder with the *em7* reporter, the *fliC* reporter luminescence decreases considerably between 2 and 9 hpi (Fig. 2*D*). At all time points, however, the level of *fliC* reporter luminescence remains significant above background (Fig. 2*D*). These data appear to be consistent with the observation made by Snyder *et al.* (8) in the *in vivo* transcriptome study, where, over the course of a 10-day UPEC infection, *fliC* transcription is down-regulated. To further substantiate these findings, we isolated total RNA from the bladders of mice that were infected for 2 and 9 h with CFT073, prepared gene-specific (*fliC* and *gapA*) cDNA, and then determined the differences in *fliC* transcription using comparative qPCR. As expected, the level of *fliC* transcription was $\log_2$ 2.8-fold (7.0-fold) less at 9 hpi compared with 2 hpi and directly correlated with the drop in *fliC* reporter luminescence from 2 to 9 hpi (Fig. 2*E*).

Despite the drop in total *fliC* reporter luminescence in the bladder between 2 and 9 hpi, a more pronounced trail of luminescence leading from the bladder to the kidneys emerged at 5 hpi and was maintained up to 9 hpi (similar to the trail observed with the *em7* reporter during ascension and early colonization of the kidneys). This phenomenon was also observed with the remaining 18 infected mice (for at least one time point between 5 and 9 hpi) and is illustrated with two additional representative mice in Fig. 2*B*. Because the trail of signal emerged at 5 hpi, it also correlated with a significant increase in *fliC* reporter luminescence over background in one or both kidneys (Fig. 2 *A* and *B*). In fact, the amount of luminescence at all time points after 5 hpi in the kidneys (with the exception of the 7-h time point in the left kidney) is significantly greater than background (Fig. 2*C*). Altogether, these data demonstrate the temporospatial expression of flagellin (and presumably flagella) during ascending UPEC infection, and that the expression of *fliC* coincides with the ascension of UPEC to the upper urinary tract.

Reassessment of the Contribution of Flagellin During Ascending Murine UTI Using an Intraurethral Challenge Method. Because *fliC* expression appeared to coincide with the ascension of UPEC from the bladder to the kidneys, we hypothesized that flagella must be playing a more important role during urinary tract ascension than what has been previously observed by our laboratory and others. It has been debated that the current methods of transurethral inoculation (using a 20- to 50-μl volume) used by our laboratory and several others results in minimal to substantial vesicoureteral reflux (that is, leakage of bacteria from the bladder into the ureters and kidneys due to the pressure or volume of the inoculum) (25). In fact, we confirmed that our method of transurethral inoculation results in minimal to no vesicoureteral reflux, as determined by viable counts present in the kidneys and biophotonic imaging after 5-min postinoculation (SI Fig. 7). Because flagella are presumed to be important for ascension of the bladder through the ureters to the kidneys, we then wanted to rule out the effect of inoculation on development of kidney infection. Therefore, we reassessed the contribution of flagellin during ascending UTI by inoculating a smaller volume (10 μl) and concentration (10^7 cfu) directly into the urethra (instead of the bladder). For comparison, the ID_{50} for transurethral inoculation is 10^6 cfu per mouse. Hopkins *et al.* (18) previously demonstrated that with this method of intraurethral challenge, vesicoureteral reflux could be avoided. Specifically, 10^7 cfu of wild-type CFT073 and CFT073 $\Delta fliC$ were independently inoculated into the urethras of eight mice per each time point. After 6 and 48 hpi, cfu/gram of bladder, kidney, and spleen tissue (for the 48-h time point only) were determined. Both the wild-type and *fliC* mutant were recovered in equal numbers from the bladder at 6 hpi, suggesting that both strains were equally able to colonize the bladder at early time points of infection (Fig. 3*A*). In contrast, the *fliC* mutant was recovered in significantly lower numbers than wild-type in both the left and right kidneys at 6 hpi ($P = 0.002$ and 0.021, respectively), thus demonstrating that the *fliC* mutant was less able to colonize the kidneys (Fig. 3*A*). At 48 hpi, the *fliC* mutant was also recovered in significantly lower numbers than wild-type
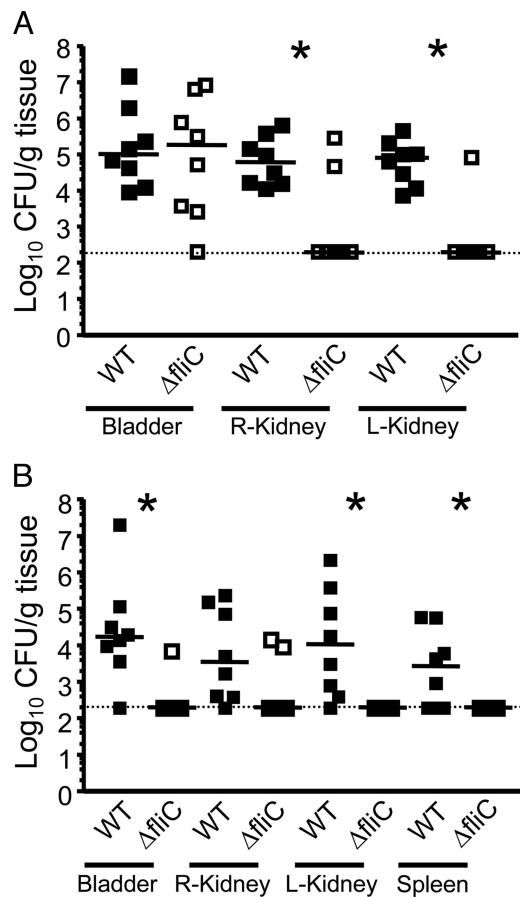
Fig. 2. Biophotonic imaging of wild-type CFT073 P$_{em7}$-*lux* and P$_{fliC}$-*lux* reporter luminescence during ascending UTI and confirmation of *fliC* expression *in vivo* by qPCR. (*A*) Dorsal and ventral sides of mice (*n* = 2) transurethrally inoculated with 10^9 cfu of wild-type CFT073 containing either P$_{em7}$-*lux* or P$_{fliC}$-*lux*. Mice were imaged from 2 to 9 hpi by using the IVIS 200, and luminescence was quantified in the bladder and kidneys by using Living Image software. (*B*) Additional images of mice (*n* = 2) inoculated with 10^9 cfu of wild-type CFT073 containing P$_{fliC}$-*lux*. Images are shown between 5 and 9 hpi to further demonstrate the trail of signal produced by the *fliC* reporter during ascension to the upper urinary tract. The scales for ventral and dorsal luminescence are the same as those shown for *A*. (*C* and *D*) Scatter plots depicting luminescence over time for P$_{fliC}$-*lux* (*n* = 19 mice), P$_{em7}$-*lux* (*n* = 20 mice), and P$_{neg}$-*lux* (*n* = 15 mice). Each data point represents either the median or log$_{10}$ median luminescence emitted from the bladder (*D*) and individual kidneys (*C*) of 14–20 CBA/J mice during specific times after inoculation. Significance of *fliC* gene expression over background at each time point was assessed by using a Mann–Whitney test. *, $P < 0.05$; ■, P$_{em7}$-*lux*; ▲, P$_{fliC}$-*lux*; and ○, P$_{neg}$-*lux*. (*E*) qPCR analysis of *in vivo* *fliC* transcription by the P$_{fliC}$-*lux* reporter. The black bar represents the log$_2$-fold change in *fliC* expression between 2 and 9 hpi during bladder colonization (*n* = 20 mice). The error bar represents the standard error of the mean.

from the bladder, left kidney, and spleen (*P* = 0.006, 0.004, and 0.037, respectively) and tended to be less well recovered than wild-type from the right kidney (Fig. 3*B*; *P* = 0.051). The 48-hpi data demonstrate that *fliC* is not only important for colonization of the kidneys but is also required for maintenance of bladder colonization and dissemination into the bloodstream.

Fig. 3. Independent challenges of mice inoculated with a 10-μl suspension of 10^7 cfu/ml of either wild-type CFT073 or CFT073 $\Delta fliC$ directly into the urethra. Eight mice were challenged for each strain and time point. At 6 hpi (*A*) and 48 hpi (*B*), bladders, kidneys, and/or spleens were harvested to determine bacterial concentrations. Each data point represents the log$_{10}$ cfu per gram of tissue collected from one mouse. Horizontal bars represent the median values of the populations. The limit of detection of this assay is 2×10^2 cfu per gram, as indicated by the dotted line. Significant differences in colonization between the wild-type and *fliC* mutant were determined by using a Mann–Whitney test. *, $P < 0.05$; ■, wild type (WT); □, $\Delta fliC$.

Discussion

Here, we describe the use of biophotonic imaging for visualization of the bioluminescent UPEC inoculum *in vivo*, for monitoring the spread of infection, and to assess the contribution of motility for this movement of the bacteria within the host. This was accomplished by measuring the level and localization of *fliC* expression *in vivo* during ascending UTI in real time. Using this technology, *fliC* expression was easily detectable over background luminescence produced by the promoterless P$_{neg}$-*lux* construct. The early decrease observed for *fliC* expression in the bladder and subsequent peak of *fliC* expression in the kidneys is intriguing, because it is coincident with the time that UPEC strain CFT073 is known to reach and colonize the kidneys (6, 26). Although it has been speculated that flagellum-mediated motility contributes to the movement of infection within the host (1, 2), the data presented in this study provide direct evidence that flagella of UPEC strain CFT073 are expressed at both the time (4–6 hpi) and location (ureters) at which UPEC ascend from the bladder to the kidneys.

Previously, our group determined the transcriptional profile of UPEC during ascending UTI by collecting urine from infected mice over an extended period (8). In that study, urine was pooled from multiple infected mice over time to allow isolation of sufficient

mRNA to measure the UPEC transcriptome (8). Although this study served as an excellent tool for identifying the transcriptional profile of the CFT073 genome during ascending UTI, it did not allow us to identify periods of transient gene expression or localize site-specific gene expression. Despite *fliC* being down-regulated in the *in vivo* transcriptome, results from cochallenge experiments conducted by our laboratory and others have demonstrated that UPEC flagella contribute significantly to fitness during colonization of the urinary tract (6, 7). Resolving this apparent paradox, biophotonic imaging for the *fliC*-luciferase transcriptional fusion revealed that wild-type UPEC express flagellin while migrating from the bladder to the kidneys. This flagellar expression during ascension to the upper urinary tract likely represents the nature of the fitness advantage seen for wild-type bacteria during the cochallenge experiments in that UPEC mutants deficient for flagellin are unable to migrate throughout the urinary tract as efficiently as bacteria expressing flagella.

To better understand the contribution of flagellin for the establishment and movement of the infection within the host, a low-dose intraurethral UTI model was used. Although the bacterial inoculum for this technique is not sufficient to generate suitable bioluminescent signal *in vivo* for localizing *fliC* expression, it was useful to evaluate the impact that deletion of the gene has on the ability of UPEC to colonize the urinary tract. Although wild-type UPEC were able to establish infection in the bladder and kidneys by 6 hpi, *fliC* mutant bacteria were able to colonize the bladder but were significantly attenuated in the kidneys at this early time point. By 48 hpi, the *fliC* mutant bacteria were attenuated in the bladder and kidneys and were not detectable in the spleen. These data provide compelling evidence that wild-type UPEC express flagellin, and presumably use flagellum-mediated motility during UTI to ascend to the upper urinary tract and disseminate within the host.

The sharp decrease in *fliC* signal within the bladder and concomitant increase in expression within the ureters and kidney that dissipates after a short time demonstrates that flagellin expression is transient *in vivo*. Consistent with our findings, Wright *et al.* (7) observed robust expression of class I flagellar genes but only minimal *fliC* (class III flagellar gene) expression within intracellular bacterial communities during development within the bladder. Recently, much attention has been focused on pattern recognition receptors that are important for proper innate immune function. Toll-like receptor 5 is known to recognize flagellated bacteria (13). Thus, bacterial pathogens such as UPEC would benefit by tightly controlling flagellar expression within the host to limit its exposure to immune defenses. It is important to know what signals are driving UPEC to switch on/off flagella expression to avoid immune responses or to ascend to the upper urinary tract and colonize the kidneys. Therefore, one could speculate that a two-component signal transduction system, such as the quorum-sensing regulators of EHEC, QseB, and QseC [involved in the transcriptional regulation of *flhDC* (27)] or other regulatory mechanisms, exists to strictly control the complex flagellar transcriptional hierarchy. Future studies investigating the effect that environmental cues and bacterial signal transduction have on *flhDC* may provide insight as to the nature of the ability for UPEC to tightly control flagellin expression *in vivo*.

Materials and Methods

Bacterial Strains, Plasmids, and Culture Conditions. Bacterial strains and plasmids used in this study are listed in SI Table 1. All strains were cultured on LB agar plates with appropriate antibiotics (100 μg/ml ampicillin or 25 μg/ml kanamycin) and incubated at 37°C for 18 h. Overnight broth cultures were obtained by inoculating a single colony into LB broth containing appropriate antibiotics and incubating at 37°C for 18 h with aeration.

***In Vitro* Growth and Motility Assays.** To assess growth *in vitro*, bacteria from overnight cultures were diluted 1:100 into 40 ml of

tryptone broth. Suspensions were cultured with aeration at 37°C in 125-ml flasks. For both the P_{em7}-lux and P_{fliC}-lux reporter constructs, the OD_{600} was measured, and luminescence was quantified at various time points by using a Synergy HT plate-reader operating KC4 software (Bio-Tek, Winooski, VT). Luminescent emission spectra were collected from 100-μl samples of culture contained within triplicate wells of a 96-well one-half area white polystyrene plate (Corning, Corning, NY) using a 530-nm filter with a bandwidth of 25 nm. For swimming and swarming motility studies, 50 μl of overnight cultures of wild-type CFT073 containing P_{em7}-lux or P_{fliC}-lux were reinoculated into 5 ml of sterile LB broth and incubated at 37°C with aeration to an $OD_{600} \cong 1.0$. At that point, cultures were stabbed into 0.25% tryptone agar plates [1% tryptone/0.5% NaCl, 0.25% Difco (BD, Sparks, MD) agar] by using a sterile inoculating needle or spotted (5 μl) onto the surface of modified 0.45% Eiken agar [per liter: 10.49 g of Eiken agar (Eiken Chemical, Tokyo, Japan)/3.50 g of yeast extract/7.00 g of tryptone/3.50 g of NaCl/40% D-glucose] containing 100 μg/ml ampicillin. Swimming and swarming plates were incubated for 16 h at 30°C or 37°C, respectively. After incubation, luminescence emitted from the swimming and swarming bacteria were captured by using the ChemiDoc XRS system (Bio-Rad). Further analysis was conducted to obtain density plots of the luminescence using the Discovery Series Quantity One software (Bio-Rad).

CBA Mouse Model of Ascending UTI. For biophotonic imaging, all mice were infected as described, with modification (6, 28). Female CBA/J mice (Harlan Sprague–Dawley, Indianapolis, IN) were anesthetized with ketamine/xylazine and inoculated transurethrally over a 30-s period with a 50-μl bacterial suspension delivering 10^9 cfu per mouse. To prepare the inoculum, overnight cultures (grown in the absence of antibiotic selection) were adjusted to deliver 10^9 cfu per mouse. Dilutions of each inoculum were spiral-plated by using an Autoplate 4000 (Spiral Biotech, Norwood, MA) to determine the input cfu per milliliter. For the low-dose independent challenge studies, a similar procedure was followed; however, mice were inoculated into the proximal end of the urethra over a 6-s period with a 10-μl bacterial suspension delivering 10^7 cfu per mouse. Six and 48 hpi, mice were killed by overdose with isofluarane, and the bladder, kidneys, and spleen were aseptically removed, weighed, and homogenized in sterile culture tubes containing 3 ml of PBS using an OMNI mechanical homogenizer (OMNI International, Marietta, GA). Appropriate dilutions of the homogenized tissue were then spiral-plated onto plain LB plates with or without antibiotic to determine the output cfu per gram of tissue. Statistically significant differences in colonization (with a P value <0.05) were determined by using an unpaired nonparametric Mann–Whitney test (InStat; GraphPad, San Diego, CA). All animal protocols were approved by the University Committee on Use and Care of Animals at the University of Michigan Medical School.

In Vivo Bioluminescent Imaging of Ascending UTI. For *in vivo* imaging of experimentally infected mice, hair was completely removed from both ventral and dorsal sides of the animals below the scapula including the abdominal and pelvic areas using a razor and cosmetic hair removal treatment (Veet, Reckitt Benckiser, Parsippany, NJ). Infected mice were imaged at various times after infection by using an IVIS 200 imaging system (Xenogen), as described (29). Mice were anesthetized in chambers containing 2.0% isofluorane inhalant (Baxter, Deerfield, IL). The anesthetic was sustained during imaging by using 2.0% isofluorane delivered via an IVIS manifold placed within the imaging chamber. Both the dorsal and ventral sides of the animals (as well as bladder and kidney tissue that was harvested *ex vivo*) were imaged separately for a maximum of 5 min. Mice infected with CFT073 containing the P_{neg}-lux reporter were also imaged at each time point to determine the level of background luminescent signal. Photon emissions were obtained from defined fixed regions of interest by using the Living Image software (Xenogen). Photon flux quantified for the bladders and kidneys was determined from ventral and dorsal sides of mice, respectively. The significance of P_{fliC}-lux and P_{em7}-lux reporter luminescence over background at each time point was assessed by using a Mann–Whitney statistical test (InStat; GraphPad). Immediately after the final imaging time point, mice were killed, and bladders and individual kidneys were surgically removed and homogenized to enumerate bacterial viable counts.

Additional Methods. Detailed methods, protocols, and primers for the construction of the bioluminescent reporters for the isolation of RNA and cDNA from *in vitro* and *in vivo* samples and for the comparative qPCR studies can be found in *SI Text* and SI Table 2.

1. Josenhans C, Suerbaum S (2002) *Int J Med Microbiol* 291:605–614.
2. Ottemann KM, Miller JF (1997) *Mol Microbiol* 24:1109–1117.
3. Bacheller CD, Bernstein JM (1997) *Med Clin North Am* 81:719–730.
4. Warren JW (1996) *Urinary Tract Infections: Molecular Pathogenesis and Clinical Management* (Am Soc Microbiol Press, Washington, DC).
5. Faro S, Fenner DE (1998) *Clin Obstet Gynecol* 41:744–754.
6. Lane MC, Lockatell V, Monterosso G, Lamphier D, Weinert J, Hebel JR, Johnson DE, Mobley HL (2005) *Infect Immun* 73:7644–7656.
7. Wright KJ, Seed PC, Hultgren SJ (2005) *Infect Immun* 73:7657–7668.
8. Snyder JA, Haugen BJ, Buckles EL, Lockatell CV, Johnson DE, Donnenberg MS, Welch RA, Mobley HL (2004) *Infect Immun* 72:6373–6381.
9. Lee SH, Butler SM, Camilli A (2001) *Proc Natl Acad Sci USA* 98:6889–6894.
10. Cummings LA, Wilkerson WD, Bergsbaken T, Cookson BT (2006) *Mol Microbiol* 61:795–809.
11. Andersen-Nissen E, Hawn TR, Smith KD, Nachman A, Lampano AE, Uematsu S, Akira S, Aderem A (2007) *J Immunol* 178:4717–4720.
12. Andersen-Nissen E, Smith KD, Strobe KL, Barrett SL, Cookson BT, Logan SM, Aderem A (2005) *Proc Natl Acad Sci USA* 102:9247–9252.
13. Feuillet V, Medjane S, Mondor I, Demaria O, Pagni PP, Galan JE, Flavell RA, Alexopoulou L (2006) *Proc Natl Acad Sci USA* 103:12487–12492.
14. Doyle TC, Burns SM, Contag CH (2004) *Cell Microbiol* 6:303–317.
15. Hardy J, Francis KP, DeBoer M, Chu P, Gibbs K, Contag CH (2004) *Science* 303:851–853.
16. Kadurugamuwa JL, Modi K, Yu J, Francis KP, Purchio T, Contag PR (2005) *Infect Immun* 73:3878–3887.
17. Wright JS, III, Jin R, Novick RP (2005) *Proc Natl Acad Sci USA* 102:1691–1696.
18. Hopkins WJ, Hall JA, Conway BP, Uehling DT (1995) *J Infect Dis* 171:462–465.
19. Mobley HL, Green DM, Trifillis AL, Johnson DE, Chippendale GR, Lockatell CV, Jones BD, Warren JW (1990) *Infect Immun* 58:1281–1289.
20. Chan K, Kim CC, Falkow S (2005) *Infect Immun* 73:5438–5449.
21. Galen JE, Nair J, Wang JY, Wasserman SS, Tanner MK, Sztein MB, Levine MM (1999) *Infect Immun* 67:6424–6433.
22. Soutourina O, Kolb A, Krin E, Laurent-Winter C, Rimsky S, Danchin A, Bertin P (1999) *J Bacteriol* 181:7500–7508.
23. Harshey RM, Matsuyama T (1994) *Proc Natl Acad Sci USA* 91:8631–8635.
24. Wiles S, Pickard KM, Peng K, MacDonald TT, Frankel G (2006) *Infect Immun* 74:5391–5396.
25. Johnson JR (1998) *Infect Immun* 66:6063–6064.
26. Gunther NW, IV, Snyder JA, Lockatell V, Blomfield I, Johnson DE, Mobley HL (2002) *Infect Immun* 70:3344–3354.
27. Sperandio V, Torres AG, Kaper JB (2002) *Mol Microbiol* 43:809–821.
28. Johnson DE, Lockatell CV, Hall-Craigs M, Mobley HL, Warren JW (1987) *J Urol* 138:632–635.
29. Kadurugamuwa JL, Sin LV, Yu J, Francis KP, Kimura R, Purchio T, Contag PR (2003) *Antimicrob Agents Chemother* 47:3130–3137.